

Flow Instabilities in Transonic Small-Disturbance Theory

Marc H. Williams*

Purdue University, West Lafayette, Indiana

and

Samuel R. Bland† and John W. Edwards‡

NASA Langley Research Center, Hampton, Virginia

The dynamics of unsteady transonic small-disturbance flows about two-dimensional airfoils is examined, with emphasis on the behavior in the region where the steady-state flow is nonunique. It is shown that nonuniqueness results from an extremely long time scale instability that occurs in a finite Mach number and angle of attack range. The similarity scaling rules for the instability are presented, and the possibility of similar behavior in the Euler equations is discussed.

Introduction

WITHIN the last few years several investigators^{1,2} have established that in certain Mach number and angle of attack regions the conservative solution for steady full potential flow over a two-dimensional airfoil is nonunique. This phenomenon occurs at high subsonic Mach numbers and is connected with an indeterminateness of the shock location. Typically three distinct equilibrium flows exist, each with a different lift. For example, a symmetric airfoil at zero angle of attack might have a zero lift symmetric equilibrium, an asymmetric equilibrium with large positive lift, or its mirror image with negative lift. If the airfoil is placed at a small positive angle of attack, one finds either a large positive lift, a small negative lift, or a large negative lift. None of these alternatives seems physically reasonable. Since the computed flowfields are essentially independent of the numerical scheme used, there is little doubt that the nonuniqueness is, in fact, a property of the differential equation.

The present study deals with the evolution of these anomalous flows in time. In this context, nonuniqueness of the steady state arises from a sensitivity of the final equilibrium to changes in the initial conditions or, equivalently, from the onset of instability in an equilibrium state. Previous related studies are reported in Ref. 3.

The results given in Refs. 1 and 2 are for the steady full potential equation. The present work is based on the unsteady small-disturbance approximation. This does change the equilibrium state structure of the problem somewhat but, as will be apparent from the results, does not alter the basic multiplicity of the steady solutions. The problem is addressed by pure numerical experimentation using existing time-dependent small-disturbance algorithms. The intent of the paper is to report several new dynamic anomalies of unsteady small-disturbance transonic flows, to verify the harmonic response results given in Ref. 3 (which were obtained with a slightly different algorithm) and, finally, to speculate on the physical relevance of these results. Attempts to improve the underlying physics of the mathematical model will be reported at a later date.

In the first section of the paper the airfoil and flow parameter regime studied and the numerical algorithm employed are described. The airfoil is symmetric so that at zero angle of attack one expects the steady flow to be symmetric. These symmetric flows are described in the second section, and evidence is given that they are, in fact, weakly unstable over a range of freestream Mach numbers.

The nature of the instability is mapped out in the third section. It is shown that, when the symmetric equilibrium is unstable, the flow evolves, very slowly, to either of two asymmetric equilibria, depending on the sign of the initial disturbance. The upper and lower surface shock waves, initially at the same location, split apart, one drifting downstream, the other upstream. The effect of this instability on dynamic response is then examined by imposing a harmonic pitch oscillation on the airfoil. The resulting hysteresis loops help to further clarify various anomalies observed in the past (for example, nonzero mean lift in response to oscillation about zero mean angle³).

In the fourth section the effect of the boundary layer on the flow is examined. The results of a simple numerical test indicate that a fully interactive boundary layer does not significantly alter the stability of the inviscid equilibrium states.

Description of the Flow Regime and Algorithm

The problem examined herein is an NACA 0012 airfoil at and near zero angle of attack at Mach numbers between 0.8 and 0.9. This case was chosen to correspond to Salas' earlier work on steady flow.²

All the results reported herein were generated with the conservative, time-accurate, small-disturbance program XTRAN2L,⁴ developed at NASA Langley. This program is a modification of LTRAN2-NLR,⁵ which includes: 1) the ϕ_{tt} term in the wave equation using the Rizzetta-Chin algorithm,⁶ 2) nonreflecting far-field boundary conditions,⁷ and 3) a "monotone" difference switch to eliminate expansion shocks.⁸

The program was run with the NLR coefficients in the wave equation, without the Krupp scaling in the vertical direction, on an 80×40 grid (the default XTRAN3S xz grid).

Since the present results are based on the small-disturbance approximation, they are subject to transonic similarity rules. Hence, most of the conclusions can be applied directly to any member of the 00XX series of airfoils. These scaling transformations are discussed in the Appendix.

Received Feb. 19, 1984; revision received Nov. 7, 1984. Copyright © American Institute of Aeronautics and Astronautics, Inc., 1985. All rights reserved.

*Associate Professor, School of Aeronautics and Astronautics, Member AIAA.

†Aerospace Technologist, Unsteady Aerodynamics Branch, Associate Fellow AIAA.

‡Head, Unsteady Aerodynamics Branch, Member AIAA.

Symmetric Flow Results

A baseline series of calculations was performed with the airfoil held fixed at zero angle of attack in a uniform freestream with Mach number ranging from 0.81 to 0.86. In the first run, the airfoil was "turned on" in a uniform stream at $M=0.81$, and the flow was allowed to develop to a steady state. This simulation spanned some 60 chords of travel (about 600 time steps). In the second run, the Mach number was reset to 0.82, and the calculation continued from the 0.81 steady state until a new steady state was achieved. This process was repeated in Mach number increments of 0.01 to $M=0.86$. In each successive simulation, the flow appeared to reach a symmetric equilibrium in from 10 to 20 chords of travel. The resulting steady pressure distributions are shown in Fig. 1.

In reality, however, these calculations would not all converge to a symmetric equilibrium if continued indefinitely. If the apparently converged solution at $M=0.85$, for example, is restarted with a large time step (corresponding to 2 chords of travel per step), the lift diverges exponentially, as shown in Fig. 2. In this case the lift history is, approximately,

$$C_L = C_{L_0} e^{st}$$

where C_{L_0} is of order 10^{-12} (since the initial asymmetry is a result of truncation error), and the growth rate s is roughly $0.01U/c$ (U =freestream velocity, c =chord). These numbers explain why the instability was not observed in the original calculation: the initial flow asymmetry is exceedingly small, and its time constant is large compared to the time scale for equilibration to the new Mach number. In fact, it would take over 2000 chords of travel for lift coefficients on the order of 0.001 to develop, given the present initial conditions.

It is important to note that the same growth rate is observed regardless of the time step (a large step is necessary only to capture a significant growth in a reasonable computational time). If the instability were numerical in origin, the growth rate would depend on Δt . We conclude that the instability must be a property of the differential equation.

In order to examine the long time evolution of these unstable flows, it is clearly desirable to introduce a controllable disturbance rather than to rely on truncation errors.

Pulse Responses

The stability of the symmetric equilibria described in the previous section was tested as follows: Starting from the symmetric flow, the airfoil was pitched up to $1/4$ -deg angle of attack and back to zero with a slow Gaussian pulse. The

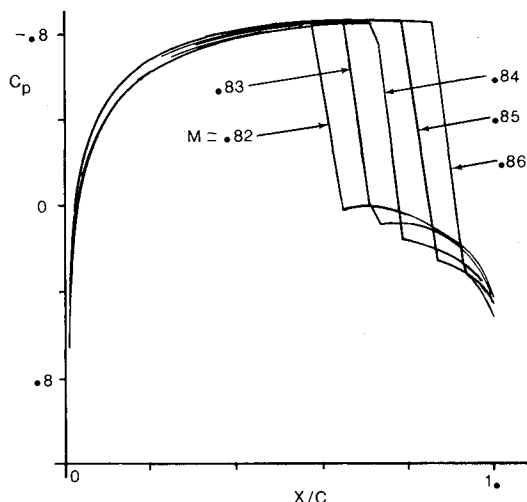
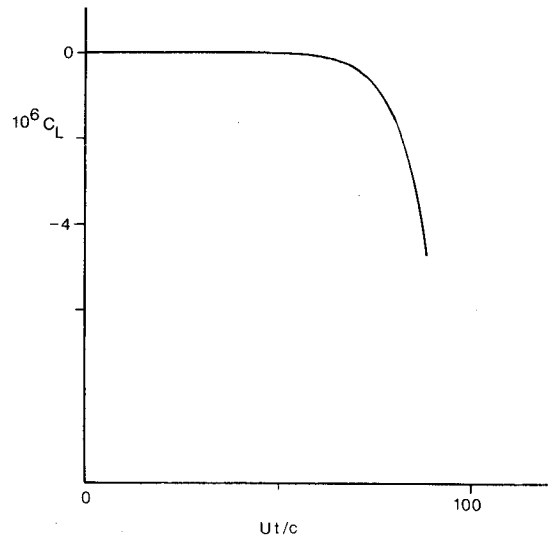


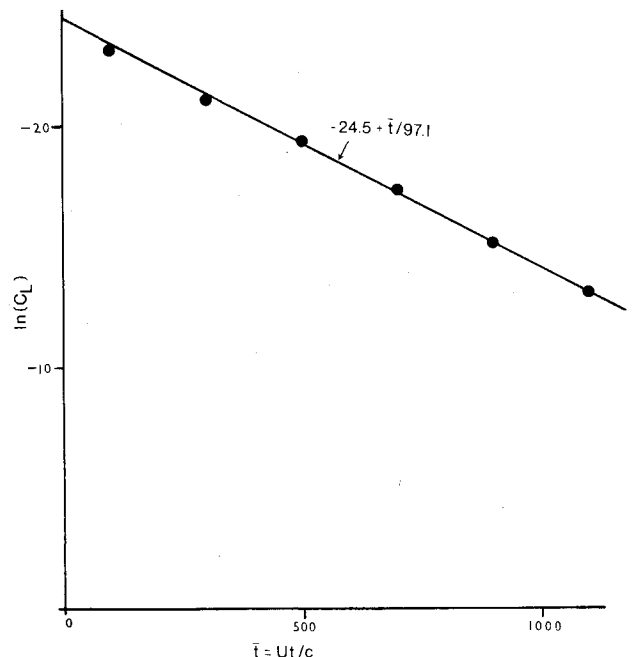
Fig. 1 Symmetric steady flow pressure distributions at $\alpha=0$ deg.

half-width of the pulse was 40 and the time step 2 chords traveled—so that the pulse duration is comparable to the instability time scale and the time increment is small enough to resolve the disturbance and long enough to give the postpulse history in a reasonable number of steps.

The resulting dynamic lift responses are shown in Fig. 3 for Mach numbers 0.82 to 0.86. It is clear from these results that the symmetric state is stable at $M=0.82$, 0.83, and 0.86—the disturbance generated by the pulse dies out in time, and the flow returns to its original symmetric zero lift condition. At Mach numbers between 0.83 and 0.86, though, the symmetric flow is unstable—the positive pulse in angle of attack induces a transition to an asymmetric equilibrium state with positive lift (a negative pitch pulse would, of course, cause a transition to a mirror image negative lift state). The pressure distribution in the asymmetric equilibrium at $M=0.84$, $\alpha=0$ is shown in Fig. 4. Clearly the large lift is caused by a large shift in the upper/lower surface shock positions from their common symmetric state locations. Aside from the shock displacement, there is very little change in the flow.



a) Time history of lift.



b) Instability growth rate.

Fig. 2 Exponential divergence of lift at $M=0.85$, $\alpha=0$ deg.

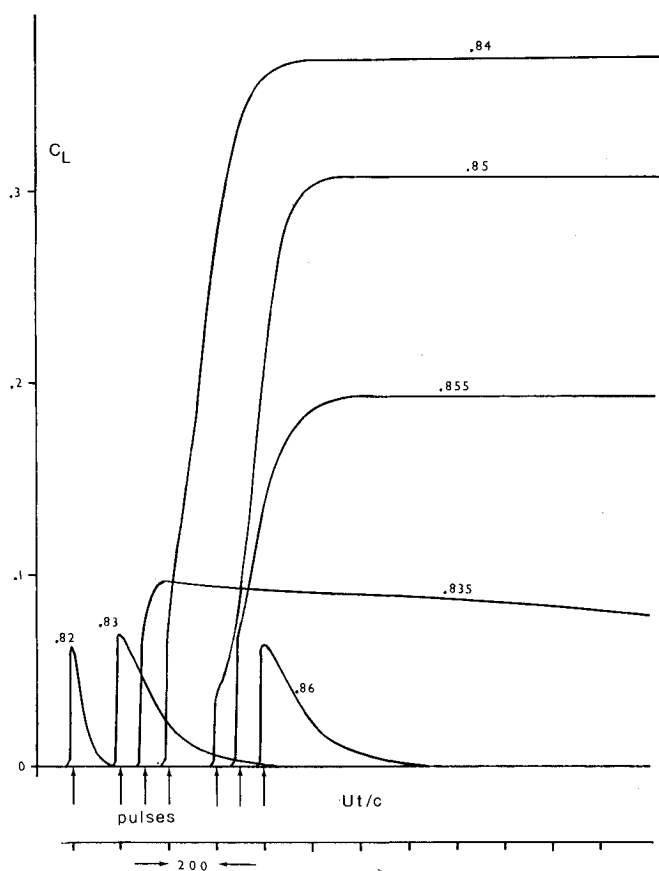


Fig. 3 Time histories of lift due to a pulse in angle of attack of $1/4$ deg for several Mach numbers.

Equilibrium lift and shock position results over the Mach number range of instability are shown in Figs. 5 and 6, respectively (each circled point was obtained by a pulse response calculation; starred points were taken from the initial symmetric flowfields).

These figures show that at zero angle of attack there are three equilibrium flowfields at any Mach number between 0.835 and 0.858. The symmetric state is unstable, and the two asymmetric states are stable (with respect to infinitesimal disturbances). Note further that the shocks cannot stand symmetrically anywhere between 72 and 88% chord. These limits are of interest because they are universal within the 00XX family of airfoils (x_s/c is a valid transonic similarity parameter). It is important to observe as well that the asymmetric equilibrium states are not always associated with shocks standing near the trailing edge (as in Fig. 4). Indeed, near the lower bifurcation Mach number, the stable shock positions are very close to the unstable symmetric location and well upstream from the trailing edge. Hence, purely numerical problems associated with trailing-edge shocks, while perhaps an issue, are not an explanation of the phenomenon.

Harmonic Responses

One of the more important applications of small-disturbance theory is the evaluation of the fluctuating aerodynamic forces that result from airfoil oscillation. Here we shall examine what happens to these forces when the airfoil is oscillated harmonically in pitch about zero angle of attack with a freestream Mach number in the range of instability.

The harmonic response characteristics depend on the amplitude of the oscillation, the reduced frequency, $k = \omega c/U$, and, sometimes, on the way the oscillation is started. Figure 7 illustrates this, for the case $M = 0.85$, by means of dynamic C_L - α loops at three reduced frequencies: 0, 0.01, and 0.05.

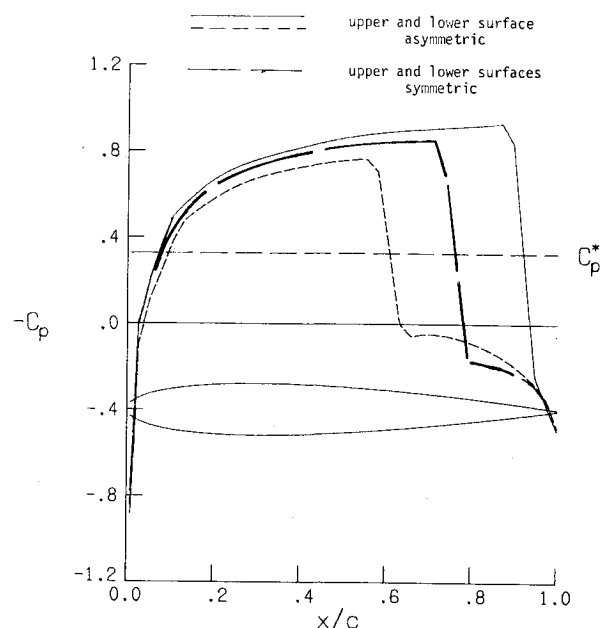


Fig. 4 Symmetric and asymmetric pressure distributions at $M = 0.84$, $\alpha = 0$ deg.

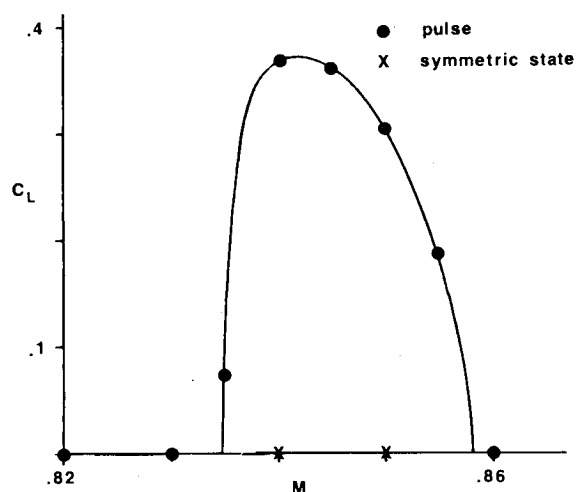


Fig. 5 Steady lift at $\alpha = 0$ deg.

The quasisteady ($k=0$) curve was obtained by a sequence of unsteady calculations (with different α) starting from the asymmetric $\alpha=0$ state labeled S in the figure. As long as $\alpha > -0.06$ deg, the computation converges to a point on the upper branch of the quasisteady curve. The lower branch is simply the mirror image of the upper, by symmetry. The middle branch, shown in dashes, is unstable and so cannot be computed with a time-accurate algorithm. The quasisteady curve is qualitatively similar to that obtained by Salas² using a conservative full potential code. (He was also able to fill in the middle branch by using an inverse steady solver.)

A harmonic oscillation in α at an *infinitesimal* reduced frequency would lead to one of two results:

1) If the amplitude were less than 0.06 deg, the flow would track the upper equilibrium curve (centered at S) or the lower curve, depending on initial conditions.

2) If the amplitude were larger than 0.06 deg, the flow would transition between the upper and lower branches during the cycle, resulting in a hysteresis loop with abrupt jumps at $\alpha = \pm 0.06$ deg.

Recall that the instability time scale is on the order of $100c/U$. Hence, the quasistatic hysteresis loop just described

would be seen only at reduced frequencies $k \ll 0.01$. The loop at $k=0.01$ for a $1/4$ -deg amplitude oscillation is shown in Fig. 7. In this case the flow does transition back and forth between the two stable branches, although with considerable lag because the oscillation period is comparable with the instability time scale. Note that the mean lift is zero. At $k=0.05$ (again for a $1/4$ -deg amplitude) the period is small compared to the instability scale. In consequence, the flow does not have time to transition between branches during the cycle. The lift loop shown in Fig. 7 remains near the upper branch because the computation was begun on the upper branch. If the initial state had been chosen on the lower branch, the final steady-state oscillation would have been about the lower branch. Presumably any initial condition with $k=0.05$ will eventually produce either the loop shown in Fig. 7 or its image. Note that at this "high" reduced frequency, the mean lift is not zero. This type of result—in which a harmonic oscillation of a symmetric airfoil about zero mean angle produces a nonzero mean lift—was observed and discussed by Dowell et al.³

Boundary-Layer Effect

Experimental data⁹ for the 0012 airfoil show no unequivocal evidence for any instability of the symmetric flow at $\alpha=0$ in the Mach number range where small-disturbance theory predicts instability. One possible explanation for this failure of the theory is that the interaction between the inviscid flow and the boundary layer stabilizes the shocks in the symmetric configuration.

This hypothesis was tested with a preliminary viscous version of XTRAN2L currently being developed at NASA Langley (by James Howlett of the Unsteady Aerodynamics Branch). The model, which is based on Rizzetta's viscous modification of LTRAN2,¹⁰ couples a quasisteady, integral, turbulent boundary-layer calculation of the displacement thickness with the existing inviscid code through the surface boundary condition. Strong interaction regions at the shock and trailing edge are not included in the formulation. From the point of view of the external flow, we see an inviscid flow over an airfoil with a compliant surface, such that the surface shape adjusts to the pressure distribution (and vice versa).

The test case chosen was this:

- 1) The flowfield was initialized in the inviscid asymmetric steady state at $\alpha=0^+$, $M=0.85$.
- 2) The boundary layer was turned on and the flowfield marched forward in time, simultaneously integrating the boundary-layer and inviscid equations, with α and M fixed.

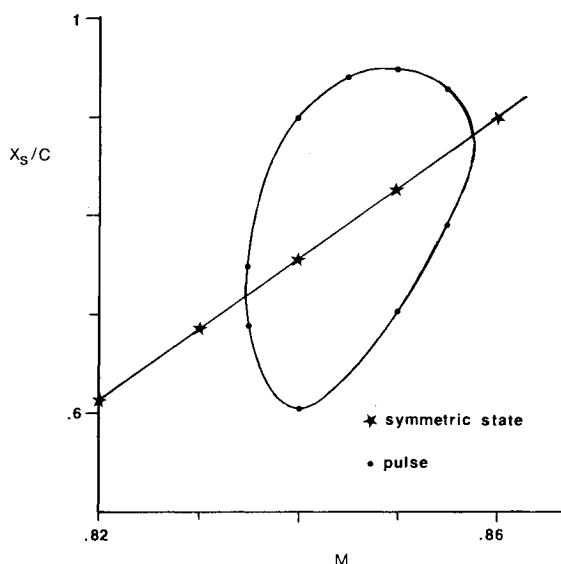


Fig. 6 Steady shock position at $\alpha=0$ deg.

Several outcomes of this test are conceivable: 1) the flow approaches a symmetric equilibrium; 2) the flow oscillates without approaching an equilibrium; and 3) the flow approaches a new asymmetric equilibrium.

The actual outcome was the third one: the boundary layer smears the shock profiles and displaces the shocks upstream but does not alter the essential asymmetry of the flow. The initial and final pressure difference distributions are shown

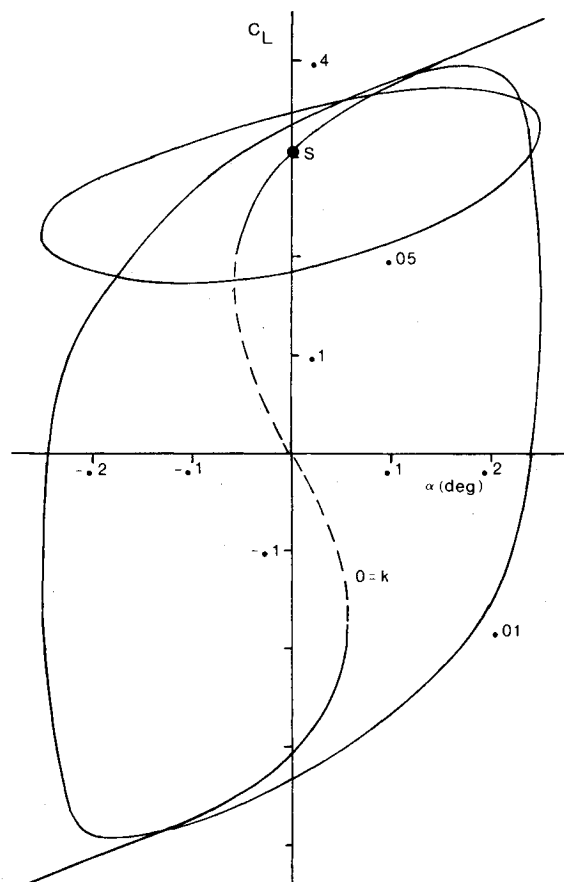


Fig. 7 Dynamic lift for simple harmonic pitching oscillation at $M=0.85$.

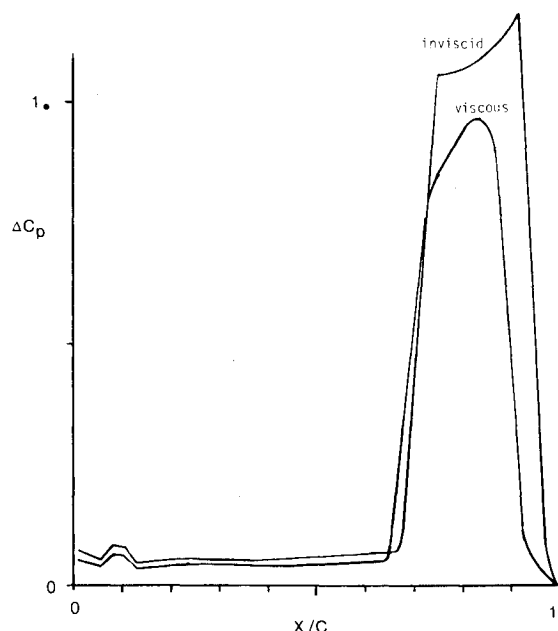


Fig. 8 Viscous effect on lifting pressure distribution at $M=0.85$.

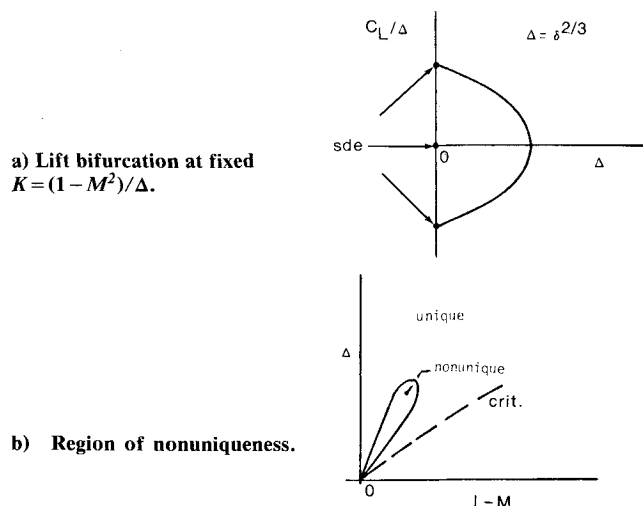


Fig. 9 Postulated behavior of steady Euler solutions at $\alpha=0$ deg.

in Fig. 8. This shift in the loading corresponds to a drop in C_L from 0.307 with no boundary layer to 0.228 with a fully adjusted boundary layer.

The transition to the new viscous equilibrium was essentially complete within 10 chords of travel. As a precaution the calculation was continued to over 100 chords with no significant change.

Although the particular boundary-layer model used in this calculation has several theoretical shortcomings, it is difficult to imagine that a more refined model would alter the basic conclusion: including boundary-layer interactions in the small-disturbance inviscid model does not cure its "unacceptable" dynamic properties.

Conclusions

The major conclusion to be drawn from the results presented here is clear: when solved as a weak conservation law, the transonic small-disturbance equation predicts flow dynamics that are physically unexpected. At lower supercritical Mach numbers there is one, stable, equilibrium state. As the Mach number increases, the original state becomes unstable and two new stable states appear. At a certain high Mach number these states recombine. This sequence appears to be unaffected by (at least a simple version of) inviscid-flow/boundary-layer interaction. Moreover, the equilibrium state structure (and presumably the dynamic response characteristics as well) is common to small-disturbance and full potential theory.

Perhaps the most surprising property of the instability is its extreme slowness—even on the time scale of upstream wave propagation. No satisfactory explanation for this long time behavior has been found, though it is clearly associated with a slow drift in the shock position.

The most pressing unresolved question is whether these anomalous flows are intrinsic to inviscid theory or simply a consequence of some approximation made in small-disturbance theory (and presumably in full potential theory as well). In this regard it is significant that both the small-disturbance and full potential theories display the anomalous behavior while Salas' solutions of the Euler equations show no conclusive evidence of it. Small-disturbance and full potential theory share a common neglect of the vorticity and entropy generated by shock waves—effects that are present in the Euler equations. Hence there is a suggestion that the shock instabilities are caused by the neglect of these mechanisms.

A more persuasive argument can be made, however, that the instabilities must arise in the Euler equations as well. Small-disturbance theory (unlike full potential theory, which

is ad hoc when shocks are present) is a rational, asymptotic limit of the Euler equations for Mach numbers near one and with small thickness ratios [$\delta \rightarrow 0$, $(1-M^2)/\delta^{2/3}$ fixed]. In the transonic scaling the Euler equations can be written symbolically as

$$N_0(U;K) = \delta^{2/3} N_1(U)$$

where U is the scaled state vector, K the transonic similarity parameter, and N_0 and N_1 nonlinear operators. If we set $\delta=0$ we get small-disturbance theory ($N_0=0$). It is difficult to imagine how the solution of the Euler equations for δ nonzero but arbitrarily small could differ substantially from the solution of small-disturbance theory.

If the solution of the Euler equations does approach the solution of small-disturbance theory as $\delta \rightarrow 0$, then the Euler equations must display the same instability and nonuniqueness properties as seen in small-disturbance theory. Since Salas' numerical results indicate that the Euler solutions are well behaved for the 0006 and 0012 airfoils, it would seem that a bifurcation must occur at some finite δ less than 0.06 (for the NACA 00XX family at zero angle of attack). This might occur as sketched in Fig. 9. Figure 9a shows a hypothetical steady-state bifurcation for a fixed K (between the limits imposed by small-disturbance theory). Figure 9b shows a hypothetical M - δ parameter map of the region of nonuniqueness in the steady Euler equations. These figures are consistent both with the present numerical results and with Salas' Euler solutions. Whether or not they in fact represent the behavior of the Euler equations, of course, awaits further investigation. If it does turn out that Fig. 9 is qualitatively correct, then either the phenomenon is real or it results from the neglect of viscous forces. In the latter event, a better model of viscous effects would be required than that used in the present investigation. In this regard it should be noted that existing experimental evidence (which is for relatively thick airfoils) does not preclude the phenomenon illustrated in Fig. 9. It is quite possible that the flow instabilities reported here do in fact occur in nature but that their domain of occurrence has simply not been studied experimentally.

Appendix: Similarity Laws for the Instability Region

Since the instability is extraordinarily weak, it should be describable, with negligible error, by the low-frequency small-disturbance equation

$$2M\phi_{xt} + (M^2 - 1 + B\phi_x)\phi_{xx} - \phi_{yy} = 0 \quad (A1)$$

where x, y are measured in units of the chord c , t in units of c/U , and B is a constant. Correspondingly, we impose the quasisteady boundary conditions

$$\phi_y = \tau f'(x) \text{ on airfoil, } 0 < x < 1, y = 0 \quad (A2)$$

$$\Delta\phi_x = 0 \text{ on wake, } x > 1, y = 0 \quad (A3)$$

where τ is a scale factor for both thickness and angle of attack.

If no external time scale is introduced through the boundary condition (e.g., if the airfoil is fixed), then the solution of the above problem must scale as

$$\begin{aligned} \phi &= (\tau/\beta)\bar{\phi}(x,\bar{y},\bar{t};K) & \beta &= \sqrt{1-M^2} \\ K &= B\tau/\beta^3, & \bar{y} &= \beta y, & \bar{t} &= \beta^2 t/M \end{aligned} \quad (A4)$$

from which it is apparent that the lift and shock positions are

$$C_L = (\tau/\beta)C_L(\bar{t};K), \quad x_S = x_S(\bar{t};K) \quad (A5)$$

Suppose that a symmetric airfoil (thickness/chord ratio τ) is at zero angle of attack. Suppose further that the flow is initially in the symmetric equilibrium state, with $C_L = 0$ and $x_S = x_{S_0}(K)$. If this flow is unstable, so that the lift grows like e^{st} , then the growth rate of the instability must scale like

$$s = (M/\beta^2)\bar{s}(K) \quad (A6)$$

Instability onset occurs when $\bar{s} = 0$, that is, for specific values of the similarity parameter K or, equivalently, at specific values of the symmetric shock position x_{S_0} . For the 0012 airfoil, with the NLR coefficient $B = M^2(2 + (\gamma - 1)M^2)$, instability appears at $M = 0.835$ and disappears at 0.858. These limits correspond to $K_1 = 1.144$, $x_{S_0} = 0.72$, and $K_2 = 1.496$, $x_{S_0} = 0.88$, respectively. Hence, for any airfoil 00τ , with any coefficient B , the symmetric flow will be unstable whenever $B\tau/\beta^3$ is between K_1 and K_2 or, equivalently, whenever the symmetric shock lies between 0.72 and 0.88. When the instability occurs, the flow will transition to a new asymmetric equilibrium, the lift and shock positions of which can easily be calculated from Eq. (A5) and Figs. 5 and 6.

A puzzling feature of the numerical results is the extremely slow growth rate of the instability, which has a time scale $t \sim 100$. This is not explained by the scaling law since in the middle of the unstable region ($M = 0.85$), the scaled time is $\bar{t} \sim 33$. We give here a simple ad hoc model of the instability, based on the scaling law and the computed equilibrium shock locus (Fig. 6), which does predict the correct growth rates.

Suppose that the shock velocity is governed by the differential equation

$$\frac{dx_S}{dt} = -A \frac{\beta^2}{M} (x_S - x_{S_0} - b)(x_S - x_{S_0})(x_S - x_{S_0} + b) \quad (A7)$$

so that x_{S_0} is the symmetric equilibrium position and $x_{S_0} \pm b$ are the asymmetric equilibria. By similitude, b and A must be determined by x_{S_0} . Note that if A is positive, the symmetric state is unstable and the two asymmetric states are stable. Linearizing about the symmetric state, we find the behavior,

$$x_S \approx x_{S_0} + Ce^{st} \quad (A8)$$

where

$$s = AB^2\beta^2/M \quad (A9)$$

From Fig. 6 the maximum value of b is 0.15 at $M = 0.845$, which yields a maximum growth rate of $0.008A$. This value

agrees with the observed growth rate if A is of order 1. Over the range of instability, then, we expect growth rates given by the empirical relation

$$s = 2.5(\beta^2/M)(x_{S_0} - 0.72)(0.88 - x_{S_0}) \quad (A10)$$

(which comes from fitting a parabola for b^2 to the results of Fig. 6).

This derivation is, of course, quite crude since Eq. (A7) has no justification beyond its consistency with Fig. 6 and the scaling laws. What has been shown is that the small growth rates observed arise "naturally," without large non-dimensional factors being inserted arbitrarily. A rational analysis of the growth rate would require solving the eigenvalue problem which results from linearizing Eqs. (A1-A3) about the symmetric equilibrium. Even if this were done, though, the cause of the instability would probably remain as mysterious as it is now.

References

- ¹Steinboff, J. and Jameson, A., "Multiple Solutions of the Transonic Potential Flow Equation," *Proceedings of the AIAA 5th Computational Fluid Dynamics Conference*, Palo Alto, CA, June 1981, pp. 347-353.
- ²Salas, M. D., Jameson, A., and Melnik, R. E., "A Comparative Study of the Nonuniqueness Problem of the Potential Equation," AIAA Paper 83-1888, July 1983.
- ³Dowell, E. H., Ueda, T., and Goorjian, P. M., "Transient Decay Time and Mean Values of Unsteady Oscillations in Transonic Flow," *AIAA Journal*, Vol. 21, Dec. 1983, pp. 1762-1764.
- ⁴Whitlow, W., "XTRAN2L: A Program for Solving the General-Frequency Unsteady Transonic Small Disturbance Equation," NASA TM 85723, Nov. 1983.
- ⁵Houwink, R. and van der Vooren, J., "Improved Version of LTRAN2 for Unsteady Transonic Flow Computations," *AIAA Journal*, Vol. 19, Aug. 1980, pp. 1008-1010.
- ⁶Rizzetta, D. P. and Chin, W. C., "Effect of Frequency in Unsteady Transonic Flow," *AIAA Journal*, Vol. 17, July 1979, pp. 779-781.
- ⁷Kwak, D., "Nonreflecting Far-Field Boundary Conditions for Unsteady Transonic Flow," *AIAA Journal*, Vol. 19, Nov. 1981, pp. 1401-1407.
- ⁸Engquist, B. E. and Osher, S. J., "Stable and Entropy Satisfying Approximations for Transonic Flow Calculations," *Mathematics of Computation*, Vol. 34, Jan. 1980, pp. 45-75.
- ⁹"Experimental Data Base for Computer Program Assessment," AGARD-AR-138, 1979.
- ¹⁰Rizzetta, D. P., "Procedures for the Computation of Unsteady Transonic Flows Including Viscous Effects," NASA CR-166249, Aug. 1981.